Calculation of Superalloy Phase Diagrams: Part IV

LARRY KAUFMAN AND HARVEY NESOR

Explicit descriptions of the Fe-Mo, Fe-W, Fe-Nb, W-Cr and Ti-W binary systems have been developed in line with lattice stability, thermochemical and phase diagram data. These descriptions, along with similar results derived previously, have been employed to calculate isothermal sections in the Cr-Al-Fe, Fe-Mo-Cr, Fe-W-Cr, Ni-Al-Co, Nb-Ti-W, Ti-W-Mo, Cr-W-Mo, Ni-Mo-W and Ni-W-Ti systems for comparison with experimental results. The effects of carbon impurities on miscibility gap formation in the Ti-W, Nb-Ti-W, Ti-W-Mo and Cr-W-Mo systems are discussed.

THE previous papers in this series[1-3] have demonstrated the means by which explicit descriptions of binary metallic systems can be employed to predict ternary systems. These papers, as well as previous studies[4-10] carried out along similar lines, have been used to generate a data base for describing the binary systems formed from ten technologically important metals: iron, chromium, nickel, cobalt, titanium, aluminum, carbon, niobium, molybdenum and tungsten. These metals combine to form forty-five binary systems and 120 ternary systems. In the present paper the five binary systems which have not yet been analyzed are considered, completing the set.

Subsequently, isothermal sections in nine ternary systems are computed for comparison with limited experimental sections in these systems. As before, the description of ternary solutions is synthesized directly from the binary data without any additional information using Koehler's Equation.[1-3,7-9] No ternary terms are added! Finally the effects of carbon impurities on miscibility gap formation in several binary and ternary systems are discussed in the light of the thermochemical description of this set of systems.

1. ANALYSES OF THE Fe-Mo, Fe-W AND Fe-Nb SYSTEMS

The current description of the iron-molybdenum, iron-tungsten and iron-niobium systems is displayed in Figs. 1 to 3 and Tables I to III in keeping with the available thermochemical and phase diagram data.[11-17] The convention employed in tabulating solution and compound phase parameters is identical to that employed in previous papers in this series.[1-3] Lattice stability values are identical with those employed earlier.[4,7] The starting point for the analyses of the Fe-Mo and Fe-W systems was the excellent theoretical and experimental study of the iron rich corner of the Fe-Mo, Fe-W and Fe-Mo-W systems at temperatures between 1000 K and 1900 K by Kirchner, Harvig and Uhrenius.[18] Kirchner et al.[18] characterized the fcc, bcc and liquid phases in these systems in addition to treating the compounds $Fe_{0.600}W_{0.400}$, $Fe_{0.600}Mo_{0.400}$, $Fe_{0.630}W_{0.370}$ and $Fe_{0.630}Mo_{0.370}$. For the Fe-Mo case the bcc and fcc phases were characterized as regular with interaction parameters of 4250 and 2315 cal/g.at. respectively. A value for the liquid phase was not given; however, if the liquid phase is also considered to be regular, then the bcc parameter of 4250 and the observed phase diagram[10-12] require that the liquid be ideal. If these values are used to compute the entire phase diagram, it is found that the BCC/LIQUID equilibrium is correctly predicted for iron rich compositions. However, the BCC/LIQUID equilibrium in molybdenum rich solutions is not calculated correctly. Thus (with reference to Fig. 1) an ideal liquid and a regular bcc solution with an interaction parameter of 4250 cal/g.at. results in a molybdenum-based bcc solution phase at 1820 K which is more extensive than observed. This discrepancy was of little consequence in the Kirchner-Harvig-Uhrenius analysis[18] where attention was fo-

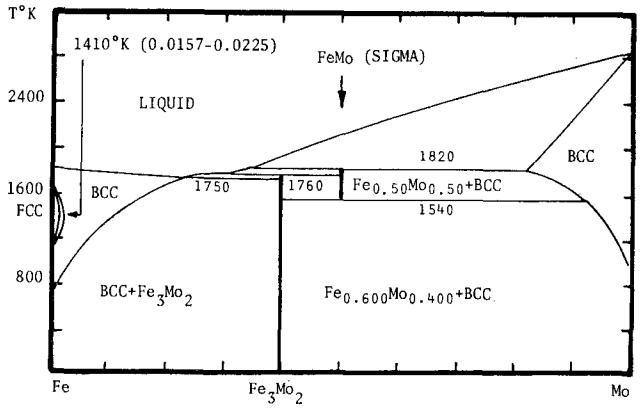

Fig. 1—Calculated iron-molybdenum phase diagram.

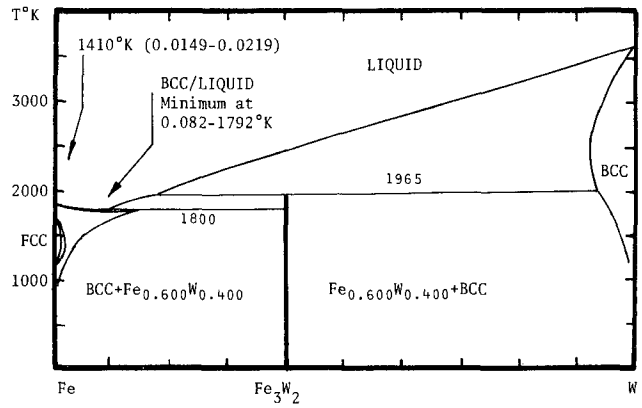

Fig. 2—Calculated iron-tungsten phase diagram.

LARRY KAUFMAN is Director of Research and HARVEY NESOR is Senior Scientist, both at Manlabs, Inc., Cambridge, Mass. 02139.

Manuscript submitted January 31, 1975.

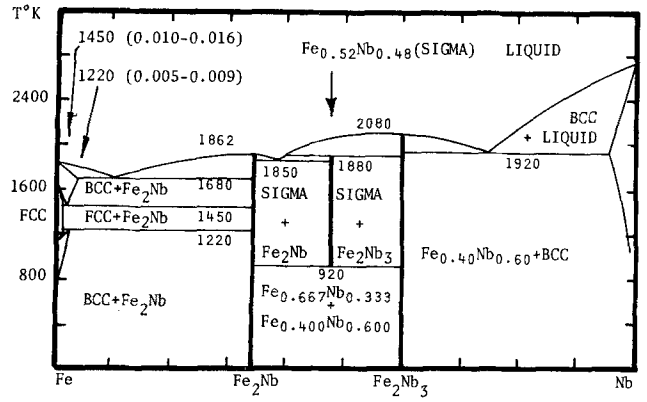

Fig. 3—Calculated iron-niobium phase diagram.

Table I. Summary of Interaction Parameters for Binary Systems (T, K, cal/g. at.) (to Convert to SI Units-Joules-Multiply by 4.184)

System		Liquid	BCC	HCP	FCC
		0	7700-2.00T	–	3125
Fe-Mo	g =	4200	8000	–	6065
Range (K)	h =	(1600 to 2900)	(800 to 2900)	–	(1000 to 1800)
	g =	4720	11200 – 2.60T	–	10100 – 3.05T
Fe-W	h =	5000	12000	–	10760 – 0.45T
Range (K)		(1700 to 3800)	(800 to 3800)	–	(1000 to 1800)
	g =	–3700	2100	–	0
Fe-Nb	h =	–7700	4000	–	0
Range (K)		(1600 to 2800)	(800 to 2800)	–	(800 to 1800)
	g =	6700	6700	–	–
W-Cr	h =	7500	7500	–	–
Range (K)		(2000 to 3700)	(500 to 3700)	–	–
	g =	3100 + 1.90T	3900 + 1.90T	6300 + 1.90T	–
Ti-W	h =	1500	3900	6300	–
Range (K)		(1700 to 3700)	(1000 to 3700)	(800 to 1200)	–

cused on the iron rich solutions; however, since the present analysis is concerned with the entire diagram, the description of Kirchner *et al.*[18] required alteration. This alteration was carried out by attempting to conform to the earlier findings[18] as closely as possible and at the same time obtaining a satisfactory description of the entire phase diagram. The final results, contained in Table I, show that asymmetrical models were required to describe the liquid, bcc and fcc solutions. However, examination of the iron rich solution parameters at 1600 K (*i.e.* in the midrange of the Kirchner *et al.*[18] analysis) yields values of 0, 4500 and 2725 cal/g.at. respectively as compared with values of 0, 4250 and 2315 cal/g.at. deduced by Kirchner *et al.*

A similar condition was encountered in the Fe-W system. Here Kirchner *et al.*[18] employed symmetrical interaction parameters of 4720, 9000 and 7800-0.54T cal/g.at. for the liquid, bcc and fcc phases respectively. Although these values reproduce the phase diagram very well on the iron rich side (which was of principal interest in the earlier study[18] the tungsten rich solubilities are in error. Thus, for example, the above noted parameters lead to a BCC + LIQUID/BCC boundary at 85 at. pct tungsten at 1900 K while the observed boundary is near 97 at. pct tungsten. Accordingly the description of Kirchner *et al.* was altered by conforming as closely as possible to their findings in iron rich solutions while attempting to obtain the best possible description of the phase diagram over

Table II. Summary of Compound Parameters for Binary Systems (T, K, cal/g. at.) (to Convert to SI Units-Joules-Multiply by 4.184)

Compound	Structure	Base	Compound Parameter (cal/g. at.)
$Fe_{0.600}Mo_{0.400}$	hR13	fcc	7800 + 1.75T
$Fe_{0.500}Mo_{0.500}$	tP30	bcc	900 + 3.00T
$Fe_{0.600}W_{0.400}$	hR13	fcc	15125 – 1.62T
$Fe_{0.667}Nb_{0.333}$	hP12	hcp	15000 + 1.50T
$Fe_{0.520}Nb_{0.480}$	tP30	bcc	
		below 1200 K	8.21T
		above 1200 K	13900 – 3.37T
$Fe_{0.400}Nb_{0.600}$	cF96	fcc	10700 + 4.00T

Table III. Comparison of Calculated and Observed Thermochemical Properties for Binary Compounds (T, K, cal/g. at.) (to Convert to SI Units-Joules-Multiply by 4.184)

	T, K	Pure Components	Free Energy of Formation	Heat of Formation
$Fe_{0.600}Mo_{0.400}$	973	bcc Fe, bcc Mo	+97 – 0.89T	+97
(calculated)	1573	fcc Fe, bcc Mo	–469 – 0.36T	–469
$Fe_{0.600}Mo_{0.400}$	973	bcc Fe, bcc Mo		–7 ± 150
(observed)[17]	1573	fcc Fe, bcc Mo		–430 ± 150
$Fe_{0.600}Mo_{0.400}$ (calculated)[18]	1223 to 1518	bcc Fe, bcc Mo	–1960 + 0.45T	–1960
$Fe_{0.500}Mo_{0.500}$	1500 to 1800	bcc Fe, bcc Mo	300 – 0.75T	300
(calculated)		fcc Fe, bcc Mo	412 – 0.818T	412
$Fe_{0.600}W_{0.400}$ (calculated)	1183 to 1665	fcc Fe, bcc W	–1490 + 0.45T	–1490
$Fe_{0.600}W_{0.400}$ (calculated)[18]	1333 to 1821	bcc Fe, bcc W	2254 – 12.50T +1.471Tln$T$	–
$Fe_{0.667}Nb_{0.333}$ (calculated)	298	bcc Fe, bcc Nb	–3180 – 0.33T	–3180
$Fe_{0.667}Nb_{0.333}$ (calculated)	1300	fcc Fe, bcc Nb	–4240 + 0.69T	–4240
$Fe_{0.667}Nb_{0.333}$ (estimated)[21]	298	bcc Fe, bcc Nb	–	–3660
$Fe_{0.667}Nb_{0.333}$ (observed)[15]	1300	fcc Fe, bcc Nb	–4350(±400) +0.91(±0.25)T	–4350 ± 400
$Fe_{0.520}Nb_{0.480}$ (calculated)	300 to 1200	bcc Fe, bcc Nb	–1440 – 2.05T	–1440
$Fe_{0.520}Nb_{0.480}$ (calculated)	1200 to 1800	fcc Fe, bcc Nb	–4910 + 0.84T	–4910
$Fe_{0.400}Nb_{0.600}$ (calculated)	298	bcc Fe, bcc Nb	–2120 – 1.07T	–2120
$Fe_{0.400}Nb_{0.600}$ (calculated)	1300	fcc Fe, bcc Nb	–2740 –0.45T	–2740

the entire range. Reference to Table I shows that the present iron rich parameters for the liquid, bcc and fcc phases in the Fe-W system at 1600 K of 4720, 7040 and 5300 are close to the above mentioned values of 4700, 9000 and 7080 derived by Kirchner *et al.* The calculated "gamma-loop" compositions derived in the present analysis conform with those measured by Kirchner *et al.* to within 0.1 at. pct over the entire temperature range of the gamma-loop (*i.e.* range of stability of fcc iron).

The current descriptions of Fe-Mo and Fe-W compound phases contained in Table II are employed to calculate the free energies and heats of formation listed in Table III and compared with recent measurements of Spencer and Putland[17] and the earlier analysis.[18] For the case of $Fe_{0.600}Mo_{0.400}$, hR13,[16] the free energy of formation at 1500 K (from bcc Fe and bcc Mo) is –1232 cal/g.at. according to the current analy-

sis, *vs* −1285 in the previous study.[18] These results are in very good agreement. However, the present calculated heats of formation at 973 K and 1573 K for this same compound are in much better agreement with recent measurements[17] shown in Table III than the result calculated in the earlier analysis.

In spite of the differences between the current analysis and the earlier results of Kirchner *et al.*,[18] both studies show that the Fe-Mo and Fe-W systems are characterized by positive heats of mixing and compounds of low stability. This is in keeping with the very small heats of formation measured by Spencer and Putland[17] and the wide two-phase BCC + LIQUID fields exhibited in both systems.

The description of the Fe-Nb phase diagram given in Tables I and II generates the phase diagram shown in Fig. 3. The latter is in good agreement with observed phase diagram data.[12,13,15,16] Table III summarizes the calculated thermochemical properties of Fe-Nb alloys. Comparison of the calculated and observed[15] values for $Fe_{0.667}Nb_{0.333}$ at 1300 K yields good agreement. However, it should be noted that the *observed* value shown for this compound is one-third the value given in Hultgren's review.[15] This is due to an error in the review which tabulated the molar properties of the compound (Fe_2Nb) under the heading of $Fe_{0.667}Nb_{0.333}$ The error can be seen by examining the original references[19,20] which reported the measurements. This has been verified by the present authors through direct communication with R. Hultgren. Table III also contains the independent estimate of the heat of formation of this compound at 298 K made by Chart and Kubaschewski[21] for comparison with the result of the present calculation. The agreement here is quite reasonable. Finally Hawkins[22] has calculated the activity of niobium at 1300 K in an iron-niobium alloy containing 0.7 at. pct niobium which corresponds to the composition at the FCC/FCC + Fe_2Nb boundary as shown in Fig. 3. Hawkins[22] derives a value for the activity coefficient of niobium equal to 2.1 from emf measurements on an alloy containing 30 at. pct Nb which is in the two-phase field. Since the free energy difference between fcc and bcc niobium[4] is 2150 + 0.80T and Table I describes the fcc as an ideal solution, the calculated activity coefficient for niobium in the fcc phase at 1300 K and 0.7 at. pct niobium is 3.5.* The difference between the calculated and observed values is well within the uncertainty of the measurement.

*See Note in Proof.

2. ANALYSIS OF THE Cr-W AND Ti-W SYSTEMS

The final binary systems to be considered are the Cr-W and Ti-W systems shown in Figs. 4 and 5. These systems are characterized by miscibility gaps in the BCC phase. The description of the solutions shown in Table I generates the phase diagrams in Figs. 4 and 5. These calculated diagrams are in excellent agreement with the observed Cr-W[11,23] and Ti-W[23,24] phase diagrams. The Ti-W case is particularly interesting since early versions of this system[11] showed a bcc miscibility gap with a critical temperature exceeding 2100 K so that the miscibility gap intersected the BCC plus LIQUID field. However, analysis of a series of

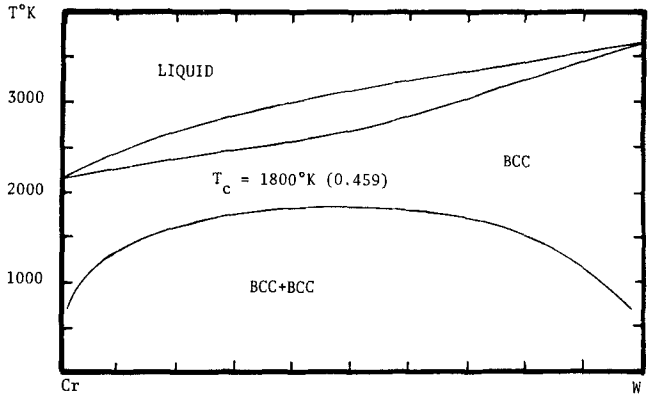

Fig. 4—Calculated chromium-tungsten phase diagram.

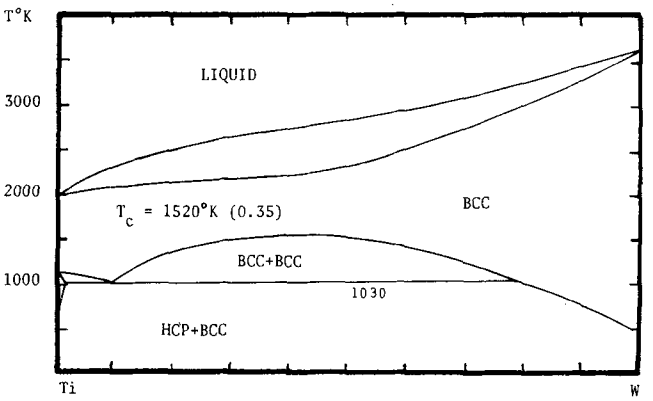

Fig. 5—Calculated titanium-tungsten phase diagram.

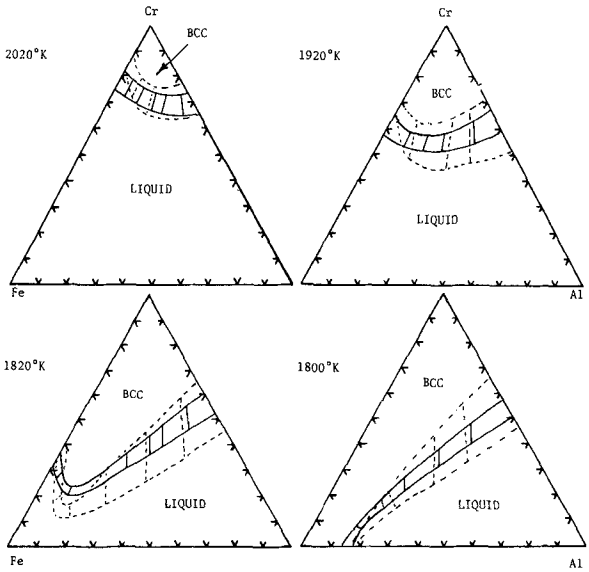

Fig. 6—Comparison of calculated and observed[25] isothermal sections in the Cr-Al-Fe system (observed boundaries are dashed).

titanium-base systems led to the conclusion that the miscibility gap critical temperature should lie well below the BCC plus LIQUID range.[4] This analysis predicted regular solution interaction parameters for the liquid, bcc and hcp phases which were equal to 8320, 7917 and 10347 cal/g.at. respectively. These values led to a critical point at 50 at. pct W near 2000 K. Subsequent redetermination of the system by Rudy and Windisch[24] placed the gap critical point

near 1520 K and 35 at. pct tungsten. The present interaction parameters for the Ti-W system shown in Table I reproduce the BCC-LIQUID, BCC-HCP and BCC miscibility gap observed in the most recent studies quite well.

The observation of lower miscibility gap temperatures in refractory metal systems over a period of years is becoming a common phenomenon. This has recently been pointed out for the case of the bcc gap in the Hf-Ta system[9] where the first measurement of the gap critical temperature was located near 2000 K.[12] Subsequent calculation[4] led to a value of T_c at 1720 K. Recent measurements (conducted more than ten years after the first experiments) put the gap maximum near 1700 K. It appears that the reduction in observed critical temperature with time of investigation is due to impurities. In particular, carbon, oxygen and nitrogen can all have such an effect in transition metal systems. The basis for this contention will be discussed in a subsequent section of this paper.

3. CALCULATION OF ISOTHERMAL SECTIONS IN THE Cr-Al-Fe SYSTEM

The chromium-aluminum-iron ternary is an important basis system for modern superalloys. Indeed the "FECRALY" alloys which offer attractive oxidation resistance and high temperature properties are based on small additions of yttrium to iron-base alloys in this system. Explicit descriptions of the component binary systems Fe-Cr,[7] Cr-Al[8] and Fe-Al[2] have been presented previously. Fig. 6 shows a comparison of calculated isothermal sections in the 1820 K to 2020 K range compared with observed sections due to Kozherov *et al.*[25] The latter is unusual in that it presents tie lines as well as phase boundaries. The agreement shown in Fig. 6 is quite remarkable. The differences on the Cr-Fe edge at high temperatures are due to the fact that the calculations reflect a higher melting point for chromium (2175 K) than the observations (2100 K).[25]

4. CALCULATION OF THE Mo-Fe-Cr SYSTEM

Figs. 6 and 7 show calculated isothermal sections in the Mo-Fe-Cr system between 923 K and 2000 K which are compared with observed sections.[26-28] The explicit descriptions of the Fe-Cr[7] and Mo-Cr[8] systems have been published previously, and the Fe-Mo case is treated in the present paper. The counterphase for the hR13 type Fe_3Mo_2 phase is hR13 type Fe_3Cr_2 defined with a bcc base and a compound parameter equal to zero. The $Fe_3(Mo, Cr)_2$ compound phase is treated as an ideal solution of the end members. Reference to Fig. 7 shows excellent agreement at 2000K between the calculated and observed section. At 1573 K the only significant difference is the extent of the sigma phase field, which must be restricted to a line in the calculations. Nevertheless, the calculated BCC/BCC + SIGMA phase boundary is in good agreement with the observed boundary.

Examination of Fig. 8 shows similar results. Apart from the extent of the sigma field, the only discrepancies between calculated and observed diagrams are the omission of the FCC field in the iron rich corner on the observed diagram at 1373 K and the miscibility gap on the Mo-Cr edge of the observed diagram at

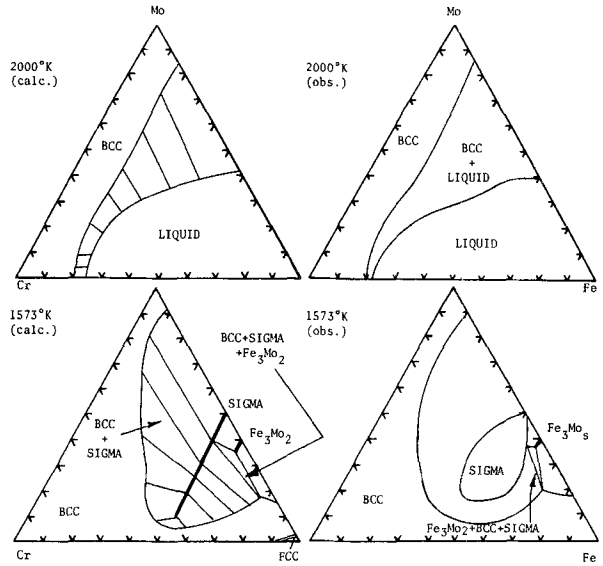

Fig. 7—Comparison of calculated and observed[26,27] isothermal sections in the Mo-Fe-Cr system.

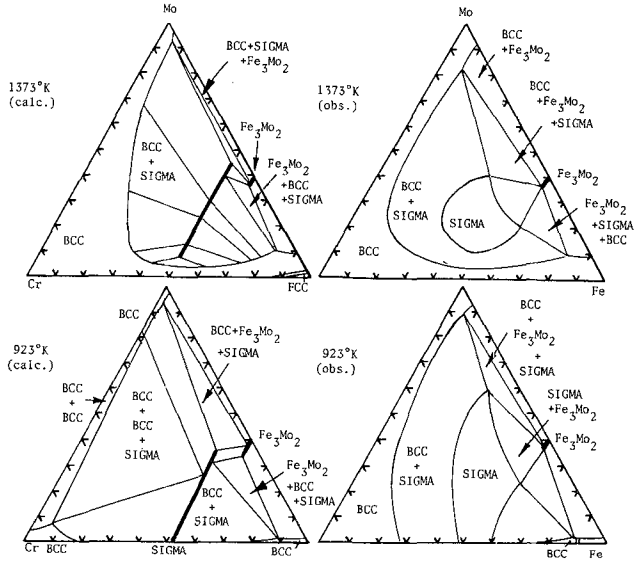

Fig. 8—Comparison of calculated and observed[27,28] isothermal sections in the Mo-Fe-Cr system.

923 K. Both these features should be present. The latter suggests that the observed section at 923 K does not represent an equilibrium diagram since sufficient time was probably not taken at 923 K in the experimental study[28] to attain equilibrium. If sufficient time were taken, a three-phase BCC + BCC + SIGMA field arising from interaction between the Mo-Cr miscibility gap and the BCC + SIGMA phase fields would result as shown in the calculated section.

5. CALCULATION OF ISOTHERMAL SECTIONS IN THE Fe-W-Cr SYSTEMS

Isothermal sections which have been calculated at 2000 K, 1725 K, 1550 K and 1375 K for the Fe-W-Cr system are compared in Fig. 9 with limited experimental results reported by Alfinitseva et al.[26] As in the case of the Fe-Mo-Cr system discussed above, the counterphase for the hR13 type Fe_3W_2 compound was taken to be hR13 type Fe_3Cr_2 characterized by C = 0 on a bcc

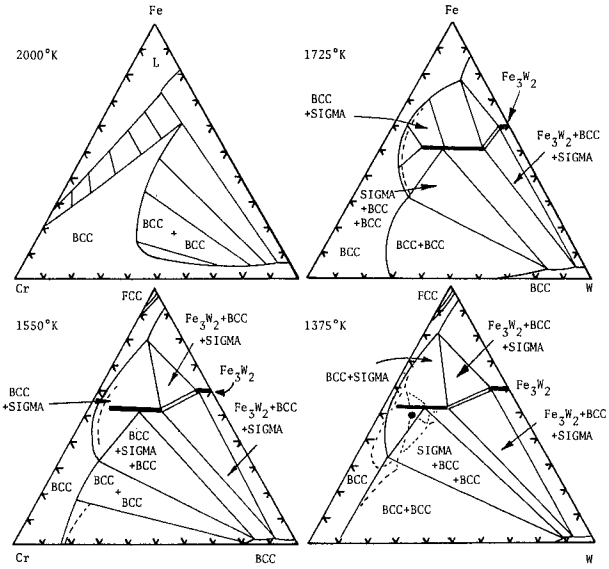

Fig. 9—Comparison of calculated and observed[26] isothermal sections in the Fe-W-Cr system. Observed phase boundaries are shown by dashed lines.

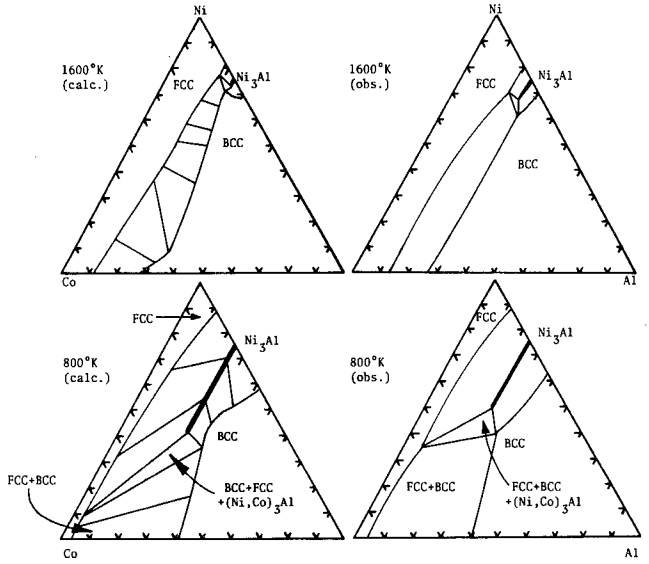

Fig. 10—Comparison of calculated and observed[29] partial isothermal sections in the Ni-Co-Al system. (The diagrams apply to the range 0 to 50 at. pct Al.)

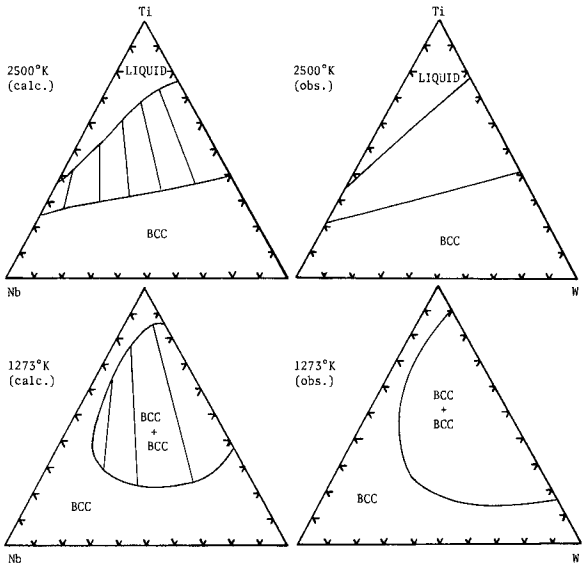

Fig. 11—Comparison of calculated and observed[30,31] isothermal sections in the Ti-W-Nb system.

base. The $Fe_3(Cr, W)_2$ compound was assumed to be an ideal solution of the components. The unstable FeW sigma phase (tP30) was defined on a bcc base with the same compound parameter as the tP30 FeMo compound. This ternary system is dominated by the positive heats of mixing which characterize the solution phases. All three binary systems have miscibility gaps in the bcc phase. These gaps are stable in Fe-Cr and Cr-W. The Fe-W miscibility gap is not stable because of the interference of Fe_3W_2. However, the Fe-W gap has the highest critical temperature of all three. Thus the calculated sections at 2000 K and 1725 K illustrate how the bcc miscibility gap spreads from the Fe-W edge to the Cr-W edge as the temperature is lowered. In addition, the sigma phase field, which is not stable in either the Fe-W or Fe-Cr edge binaries at high temperature, is stable in the center of the ternary. However, as the temperature is reduced, the sigma field moves toward the Fe-Cr edge where it ultimately becomes stable near 1100 K. Although the experimental data concerning this ternary system is quite limited, the boundaries shown by dashed curves in Fig. 9 are in general conformity with the calculations.

6. CALCULATION OF PARTIAL ISOTHERMAL SECTIONS IN THE Ni-Al-Co SYSTEM

Partial isothermal sections at 1600 K and 800 K were calculated in the Ni-Al-Co system and compared with experimental results reported by Schramm[29] in Fig. 10. The counterphase for the cP4 structure Ni_3Al was described by the Co_3Al stoichiometry characterized on a fcc base by a value of C = 0. The $(Ni, Co)_3Al$ compound phase was described by an ideal solution. The component binary systems Ni-Al,[2] Co-Al[3] and Ni-Co[7] have been described in earlier publications. However, the earlier description of the bcc phase in the Ni-Co system was limited to temperatures below 1000 K. Since definition of this phase is required in the present case above 1000 K the solution was reconsidered by retaining a symmetrical description and employing the following expression for the interaction parameter between 300 K and 1600 K.

$$g[T] = h[T] = 6527 - 2.5665T - 0.15157 \times 10^{-2} T^2 + 0.20743 \times 10^{-5} T^3 \text{ cal/g.at.} \quad [1]$$

The general agreement between the calculated and observed partial isothermal sections is quite reasonable although improvements could probably be made by introducing deviations from ideal mixing into the cP4 structure $(Ni, Co)_3Al$ compound in a manner similar to that employed for the cP4 structure $Ni_3(Al, Nb)$ compound phase.[3]

7. CALCULATION OF ISOTHERMAL SECTIONS IN THE Ti-W-Nb AND Ti-W-Mo SYSTEMS

Fig. 11 shows calculated isothermal sections at 2500 K and 1273 K which are compared with the obser-

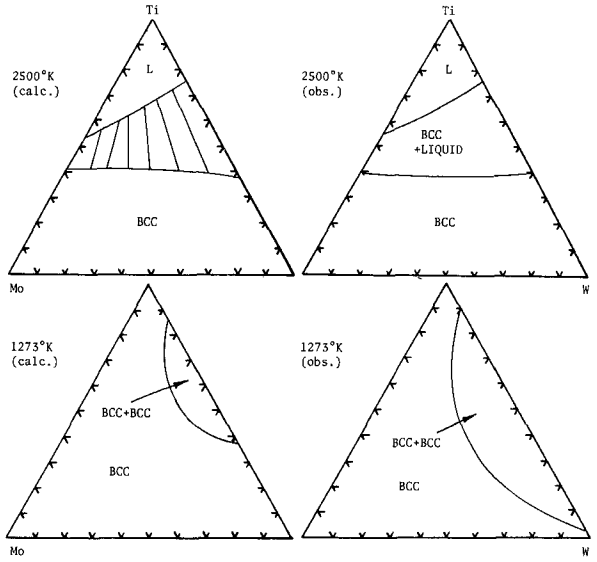

Fig. 12—Calculated and observed[32] isothermal sections in the Ti-W-Mo system.

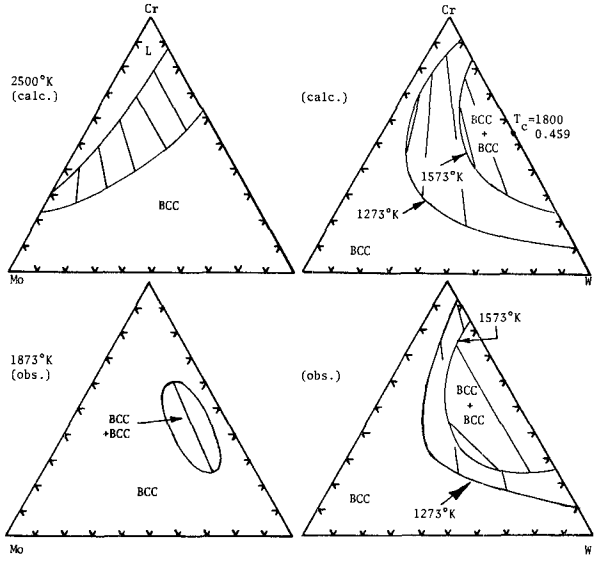

Fig. 13—Comparison of calculated and observed[35] isothermal sections in the Cr-W-Mo system.

vations reported by Bychkova, Baron and Savitski[30] and Zakharov, Novik and Daneliya.[31] The calculations were carried out on the basis of the previous descriptions of the Ti-Nb[4] and W-Nb[3] binary systems and the present description of the Ti-W system. The agreement between the computed and observed sections at 2500 K is quite good. The major difference at 1273 K is the extent of the miscibility gap on the Ti-W edge. The calculation is in accordance with the recent measurements of Rudy and Windisch[24] cited earlier while the observed 1273 K isothermal section shows a much larger miscibility gap which is characteristic of the early versions of the Ti-W system[11] discussed previously.

Fig. 12 compares the calculated sections in the Ti-W-Mo system at 2500 K and 1273 K with the observations of Zakharov and Savitski.[32] This comparison discloses the same pattern as that shown in Fig. 11; namely, that comparison of the calculated and observed BCC-LIQUID equilibrium yields good results but the observed BCC miscibility gap is much larger than the calculated gap in the ternary and on the Ti-W edge. The analysis of this ternary was carried out on the basis of the earlier study of the Ti-Mo system[4] and the current assessment of the Ti-W system. There are no thermochemical data available for the Mo-W system. Consequently the properties of this system must be estimated. The bcc phase in the Mo-W system is thought to be continuous with no miscibility gap formation. Thus, if the system is assumed regular in first approximation then the interaction parameter cannot be more positive than 2000 cal/g.at. If it were, a miscibility gap would be observed at temperatures below $T_c = 2000/2R = 500$ K. This estimate provides an upper limit for the Mo-W interaction parameter for the bcc phase. Previous calculations of the Mo-W-Os system (Ref. 4, page 238) set B = +1296 cal/g.at. A lower limit can be obtained as follows. The Zr-Mo and Zr-W systems[4] are characterized by positive heats of mixing. Both systems contain Laves phases which have small negative heats of formation. The calculated free energy of formation of $Zr_{0.333}Mo_{0.667}$ and $Zr_{0.333}W_{0.667}$ are $-2760 + 0.3T$ and $-990 + 0.3T$ cal/g.at. respectively.

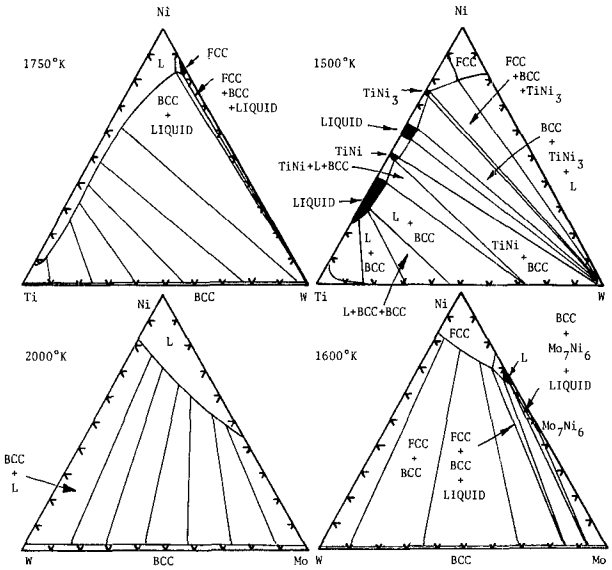

Fig. 14—Calculated isothermal sections in the Ni-W-Ti and Ni-Mo-W systems.

If we treat the compound $Zr_{0.333}Mo_{0.333}W_{0.333}$ as an ideal solution, then the free energy of this compound is one-half the sum of the free energy of formation of the components (*i.e.* $-1840 + 0.3T$ cal/g.at.) plus the entropy of mixing contribution ($\frac{2}{3}$(RT(0.5 ln 0.5 + 0.5 ln 0.5))). This means that the free energy of formation is equal to $-1840 - 0.62T$ cal/g.at. Zakharov and Savitski[33] have determined the isothermal sections in this system at 1273 K, 1873 K and 2273 K. At each of these temperatures the Laves phases form a complete set of solutions which run right across the ternary triangle. Thus if one considers the intersection of a tie line connecting Zr and $Mo_{0.5}W_{0.5}$ with the Laves phase, then

$$\tfrac{1}{3}\,Zr + \tfrac{2}{3}\,Mo_{0.5}\,W_{0.5} \rightarrow Zr_{0.333}Mo_{0.333}W_{0.333} \qquad [2]$$

since the Laves phase is stable. The free energy of formation of $Mo_{0.5}W_{0.5}$ is equal to $0.25B + RT \ln 0.5$, where B is the interaction parameter for the bcc phase.

Since Eq. [2] proceeds to the right,

$$\tfrac{2}{3}(0.25B + RT \ln 0.5) > -1840 - 0.62T \quad [3]$$

or

$$B > -11040 + 1.80T \quad [4]$$

thus at 1873 K

$$B > -7670 \text{ cal/g.at.} \quad [5]$$

A final estimate for the interaction parameter of the bcc Mo-W phase is obtained from Kirchner *et al.*[18] who cite work by Chekhovski, Tarasov and Zukova[34] as a basis for concluding that the bcc phase is ideal (*i.e.* $B = 0$). Since this value is within the estimated limit (*i.e.* -7670 to $+2000$ cal/g.at.) it was assumed in calculating the isothermal sections shown in Fig. 12 that both the liquid and bcc solid solutions in the Mo-W system are ideal.

8. CALCULATION OF THE Cr-W-Mo PHASE DIAGRAM AND THE EFFECT OF IMPURITIES ON MISCIBILITY GAP CRITICAL TEMPERATURES

The previous analysis of the Cr-Mo[8] system and the present description of the Cr-W and W-Mo systems have been used to compute the isothermal sections in the Cr-W-Mo system shown at 2500 K, 1573 K and 1273 K in Fig. 13. The calculations show a miscibility gap at low temperatures spreading from the Cr-W edge (see Fig. 4) toward the Cr-Mo edge. The Cr-Mo binary system has a miscibility gap with a critical temperature of 1153 K at a composition of 61.7 at. pct Cr.[8] The gap shrinks as the temperature increases and disappears on the Cr-W edge above 1800 K. The excess free energy of the bcc phase in the Cr-Mo system is given[8] by Eq. [6] as

$$F_E^{BCC} = x(1-x)((1-x)(8200 - 2.7T) + x(5100 - 1.4T)) \text{ cal/g.at.} \quad [6]$$

Since the W-Mo bcc phase is being considered ideal and the Cr-W bcc solution exhibits more positive deviations than those shown in Eq. 6, the calculated tie lines rotate from the Cr-W edge toward the Cr-Mo edge in keeping with the general discussion presented on page 299 of Ref. 4.

Fig. 13 also shows the experimental results of Grum-Grzhimailo and Prokofiev[35] at 1273 K, 1573 K and 1873 K. At the lower temperatures, the observed extent of the miscibility gaps is in relatively good agreement with the calculations. Strangely however, the 1573 K set of tie lines on the observed section (lower right corner of Fig. 13) rotates from the Cr-W edge toward the W-Mo edge. If this observation is correct it would imply that the deviations become more positive in the W-Mo system than in the Cr-Mo system above 1273 K. This is quite unusual. Moreover, the experimental section at 1873 K,[35] in the lower left corner of Fig. 13, shows an isolated gap. The results of Grum-Grzhimailo and Prokofiev[35] suggest a summit gap temperature near 2000 K and a critical composition near 45 at. pct Cr, 45 at. pct W, 10 at. pct Mo. This finding presents quite a contrast to the calculations and requires some discussion. In particular it is worthwhile considering the results of the Ti-W, Ti-W-Nb and Ti-W-Mo miscibility gap calculations as well since in each of these cases the observed gaps exceed the computed results. In the Ti-W case more recent measurements show a smaller miscibility gap, as noted previously. Some insight into the problem can be gained by considering the Cr-W-Mo case and simplifying the solution models employed to a regular solution approximation. If this is done in the vicinity of 1800 K to 2000 K then the interaction parameter for the bcc Cr-Mo solution is approximately 2600 cal/g.at., the Cr-W parameter is approximately 7200 cal/g.at. and the W-Mo parameter is zero. If we change the order of the elements to Mo-Cr-W in keeping with the definitions on page 299 of Ref. 4 then E_{ij} = (B Mo-Cr) = 2600; E_{ik} = (B Mo-W) = 0 and E_{jk} = (B Cr-W) = 7200 cal/g.at. These parameters can now be examined for conformity with the conditions under which an isolated miscibility gap can form (page 299 of Ref. 4).

$$T_S = -[(E_{jk} + E_{ij} - E_{ik})^2 - 4E_{jk}E_{ij}]/8RE_{ik} \quad [7]$$

$$X_S = \tfrac{1}{2} = X_{Cr} \quad [8]$$

and

$$Z_S = Z_{Mo} = (E_{ik} + E_{jk} - E_{ij})/4E_{ik} \quad [9]$$

Eqs. [7] to [9] give the summit temperature at the top of the isolated gap as well as the compositions in terms of the regular solution interaction parameter. The equations are written for the case where $E_{jk} > E_{ij} > E_{ik}$, *i.e.* (B Cr-W) = 7200 > (B Mo-Cr) = 2600 > (B Mo-W) = 0. This is the basis for changing the orientation of the elements above. Under the present conditions with $E_{ik} = 0$, no summit condition, hence no isolated gap, can exist! However, if E_{ik} (*i.e.* B Mo-W) is negative then an isolated gap will result. Unfortunately E_{ik} (*i.e.* B Mo-W) must become quite negative before an isolated gap with a T_S near 2000 K can be achieved. For example an interaction parameter of -6000 cal/g.at. leads to T_S = 1820 K and Z_{Mo} = 5.6 at. pct. More negative values are required to achieve higher summit temperatures, *i.e.* -8000 cal/g.at. leads to 1900 K and 10.6 at. pct Mo while $-10{,}000$ cal/g.at. leads to a summit at 1980 K and 13.5 at. pct Mo. Eq. [8] requires the chromium content at the summit to be 50 at. pct. Thus a regular solution interaction parameter of approximately $-10{,}000$ cal/g.at. for the Mo-W bcc solution is required to generate an isolated gap like that shown in Fig. 13. Unfortunately this value is outside the limits set in the foregoing discussion of the Ti-W-Mo system (lower limit of -7670). It is also very far removed from the result which Kirchner *et al.*[18] deduced from the observations of Chekhovski *et al.*[34] As a consequence it is useful to consider an alternative answer as follows.

If we return to the Ti-W case and consider the effects of carbon additions to the bcc phase then Eqs. [7] to [9] can be applied to the bcc phase in the C-W-Ti system. The bcc phases in the C-Ti and C-W cases have been described as regular solutions with interaction parameters corresponding to -50000 and $+4000$ cal/g.at. respectively. Fig. 5 shows that the gap critical temperature in the W-Ti system is 1520 K, but

Table I shows that the W-Ti bcc phase is not regular. If we approximate this solution by a regular solution with an interaction parameter of 6000 (to yield T_c = 1500 K), then we can apply Eqs. [7] to [9] to compute T_s. The result is T_s = 4300 K at 50 at. pct W, 24 at. pct C and 26 at. pct Ti. This isolated gap is certainly not stable, due to the compounds of high stability (*i.e.* TiC) in this ternary system. However the calculation shows that the addition of carbon (which has a large negative interaction parameter with one partner and a small positive interaction parameter with the other) can increase the gap stability considerably. This result has particular significance in understanding the reported experimental behavior in the Ti-W, Ti-W-Nb, Ti-W-Mo and Cr-W-Mo systems. In addition it may offer some insight into development of alloys which can be strengthened by spinodal decomposition through creation of miscibility gaps by deliberate impurity additions.

In conclusion, it appears that the small difference between the calculated and observed sections in Fig. 13 are mainly due to impurities (most probably carbon and/or oxygen).

9. CALCULATION OF ISOTHERMAL SECTIONS IN THE Ni-W-Ti AND Ni-Mo-W SYSTEMS

The previous descriptions of the Ni-Ti,[9] Ni-Mo[9] and Ni-W[10] systems coupled with the present ideal solution characterization of the Mo-W system have been employed to compute the isothermal sections in the Ni-W-Ti and Ni-Mo-W systems which are shown in Fig. 14. In the former case, the Ti-Ni binary exhibits much more negative deviations (*i.e.* much more negative free energies of mixing and formation) than the Ni-W or Ti-W cases. Consequently the tie lines run from the Ti-Ni binary to tungsten. In the Ni-Mo-W case, the tie lines run from the Mo-W edge toward the nickel corner since the nickel side of the Ni-W system has the most negative free energies of formation while the Ni-Mo and Mo-W edges are close to ideal. Unfortunately no experimental data could be located for comparison with the calculated results for these systems.

The Ni-W-Ti calculations were performed by treating the hP16 structure, WNi_3 counterphase of $TiNi_3$, on an hcp base with C = 0. The Ni_3(Ti, W) compound solution was assumed to be ideal. Similarly the counterphase for TiNi was taken to be a cP2 structure WNi on a bcc base with C = 0. This compound solution was also assumed to be ideal. The compound solution phase between Ti_2Ni and W_2Ni was also assumed to be ideal and based on the fcc structure. The compound parameter for the cF96 structure W_2Ni was assumed to be equal to zero. Finally, the counterphase for Mo_7Ni_6 was taken to be an oP112 structure W_7Ni_6 based on a bcc structure with C = 0. The $(Mo, W)_7Ni_6$ compound solution was assumed to be ideal.

10. SUMMARY

The broad range of systems which can now be considered by the present approach, as well as the extensive number of systems in which the calculations compare favorably with experimental measurements, provides additional support for the efficacy of the computational method. The authors hope that the examples displayed in this series of papers will lead to application of the method to solution of practical problems and stimulate future thermochemical and phase equilibrium studies in order to provide a more accurate and more extensive understanding of metallic systems.

ACKNOWLEDGMENT

This work has been sponsored by the Division of Materials Research, Metallurgy and Materials Section of the National Science Foundation, Washington, D. C., under Grant DMR-72-03233A02.

Note in Proof. The reviewer's surprise at a calculated activity coefficient of 3.5 for niobium in the ideal fcc solid solution indicates that added exposition of the present thermochemical basis is required. This is further supported by recent discussions of this subject, Ref. 36-38. The important feature in this case is the difference in crystal structure between the solution in question (fcc) and the stable form of niobium (bcc). Consequently, the activity coefficient of niobium in the fcc phase of the iron-niobium system f_{Nb}^{fcc} relative to pure bcc niobium is given by the following expression [4]:

$$RT\ln f_{Nb}^{fcc} = \Delta F_{Nb}^{bcc \rightarrow fcc} + F_E^{fcc} + (1 - x)\, \partial F_E^{fcc}/\partial x$$

In this expression R = 1.987 cal/g. at. K is the gas constant, T, K is the absolute temperature and x the atom fraction of niobium. The excess free energy of the fcc solid solution based on pure fcc iron and pure fcc niobium is F_E^{fcc}. The latter term and its derivatives are zero for an ideal solution at all values of x. Finally, $\Delta F_{Nb}^{bcc \rightarrow fcc} = 2185 + 0.85T$ cal/g. at. is the free energy difference between the bcc and fcc forms of pure niobium Ref. 4. On this basis the activity coefficient differs from unity even though the solution is ideal.

REFERENCES

1. L. Kaufman and H. Nesor: *Met. Trans.*, 1974, vol. 5, p. 1617.
2. L. Kaufman and H. Nesor: *Met. Trans.*, 1974, vol. 5, p. 1623.
3. L. Kaufman and H. Nesor: *Met, Trans. A*, 1975, vol. 6A, pp. 2115-22.
4. L. Kaufman and H. Bernstein: *Computer Calculation of Phase Diagrams,* Academic Press, New York, 1970; MIR Publications, Moscow, 1972.
5. L. Kaufman and H. Nesor: *Titanium Science and Technology,* R. I. Jaffee and H. Burte, eds., vol. 2, p. 773, Plenum Press, New York, 1973.
6. L. Kaufman and H. Nesor: *Proceedings of Conference on In Situ Composites,* vol. 3, p. 21, National Materials Advisory Board–National Academy of Sciences, Washington, D.C., Publication NMAB-308, 1973.
7. L. Kaufman and H. Nesor: *Z. Metallk.*, 1973, vol. 64, p. 249.
8. L. Kaufman and H. Nesor: *Annual Review of Material Science,* R. Huggins, ed., vol. 3, p. 1, Annual Review Inc., Palo Alto, California, 1973.
9. L. Kaufman and H. Nesor: *Treatise on Solid State Chemistry,* N. B. Hannay, ed., Plenum Press, New York, 1975, vol. 5, pp. 175-232.
10. L. Kaufman and H. Nesor: *Can. Met. Quart.*, September 1975, vol. 14, no. 3.
11. M. Hansen and K. Anderko: *Constitution of Binary Alloys,* McGraw-Hill, New York, 1958.
12. R. P. Elliot: *ibid,* first supplement, 1965.
13. F. A. Shunk: *ibid,* second supplement, 1968.
14. R. Hultgren, R. L. Orr, P. D. Anderson, and K. K. Kelley: *Selected Values of Thermodynamic Properties of Metals and Alloys,* John Wiley, 1963.
15. R. Hultgren, P. D. Desai, D. T. Hawkins, M. Gleiser, and K. K. Kelley: *Selected Values of the Thermodynamic Properties of Metals and Alloys,* American Society for Metals, Metals Park, Ohio, 1973.
16. W. B. Pearson: *Handbook of Lattice Spacings and Structures of Metals,* vol. 2, Pergamon Press, London, 1967.
17. P. J. Spencer and F. H. Putland: *J. Chem. Thermo,* 1975, vol. 7, p. 531.
18. G. Kirchner, H. Harvig, and B. Uhrenius: *Met. Trans.*, 1973, vol. 4, p. 1060.
19. G. B. Barbi: *Z. Naturforsch.*, 1969, vol. 24a, pp. 1580-85.
20. V. N. Drobyshev and T. N. Rezuhkina: *Russ. Met.*, 1966, vol. 2, pp. 85-89.
21. T. G. Chart and O. Kubaschewski: *Metallurgical Chemistry,* O. Kubaschewski, ed., p. 577, HMSO, London (SBN 11480026X), 1972.
22. R. J. Hawkins: *Chemical Metallurgy of Iron and Steel,* p. 310, Iron Steel Inst., London, (ISBN 0900497351), 1973.
23. E. Rudy: *Compendium of Phase Diagram Data,* AFML-TR-65-2, Part V, Air Force Materials Laboratory, Wright-Patterson Air Force Base, Ohio, 1969.

24. E. Rudy and St. Windisch: *Trans. TMS-AIME,* 1968, vol. 242, p. 953.
25. V. A. Kozherov, M. A. Ryss, S. E. Pigasov, V. I. Antonyenko, Yu. S. Kuznyetsov, G. G. Mikhailov, and I. Yu. Pashkyev: *Tr. Chelyabinsk Electrometallurg. Kombinata.,* 1970, vol. 2, pp. 69-76.
26. R. A. Alfinitseva, G. P. Dimitriev, V. G. Korbeynikova, V. M. Pan, V. N. Svechnikov, and A. K. Shyrin: *Sb. Nauk. Tr. Metallovie An. SSSR,* 1964, no. 20, pp. 108-24.
27. J. Putnam, R. D. Potter, and N. J. Grant: *Trans. ASM,* 1951, vol. 43, p. 824.
28. S. R. Baen and P. W. Duwez: *Trans. AIME,* 1951, vol. 191, p. 331.
29. J. Schramm: *Z. Metallk.,* 1941, vol. 33, p. 403.
30. M. I. Bychkova, V. V. Baron, and E. M. Savitski: *Svoistava Primenenie Zharoprochi Splavov,* Nauka, pp. 30-34, 1966.
31. A. M. Zakharov, F. S. Novik, and E. P. Daneliya: *Izv. An. SSSR Metally,* 1970, no. 5, pp. 212-21.
32. A. M. Zakharov and E. M. Savitski: *Izv. An. SSSR Metally,* 1966, no. 6, pp. 121-26.
33. A. M. Zakharov and E. M. Savitski: *Izv. An. SSSR Metally,* 1965, no. 1, pp. 151-59.
34. V. Ya. Chekhovski, V. D. Tarasov, and I. A. Zhukova: *Teplofiz. Vys. Temp. Moscos,* 1970, vol. 8, p. 449.
35. N. V. Grum-Grzhimailo and D. I. Prokofiev: *Zh. Neorg. Khim.,* 1962, vol. 7, p. 596 (Translation: *Russian Journal of Inorganic Chemistry,* 1962, vol. 7, p. 303).
36. G. Kirchner and B. Uhrenius: *Met. Trans. A,* 1975, vol. 6A, pp. 224-26.
37. L. Kaufman: *Met. Trans.,* 1974, vol. 5, pp. 1688-89.
38. J. Chipman: *Met. Trans.,* 1974, vol. 5, pp. 521-23.